November 05, 2007

Collagen Bioreactor

Ryan Cahill

Kelli Church

Brad Jaworski

COLLAGEN BIOREACTOR

MIMU702

Technical Design Report

Collagen Bioreactor

Final Report

Design Advisor: Prof. Jeff Ruberti

Design Team
Ryan Cahill, Kelli Church
Brad Jaworski

April 11, 2005

Department of Mechanical and Industrial Engineering
College of Engineering, Northeastern University
Boston, MA 02115

April 11th 2005

Professor J. Ruberti
365 Snell Engineering
360 Huntington Avenue
Boston, MA 02115

Dear Professor J. Ruberti,

Collagen Bioreactor Design Team is pleased to present a completed prototype of the Collagen Bioreactor, a device capable of applying load to a small tissue specimen. Included you will find a copy of the Collagen Bioreactor project.

The design provides a tensile load to a cornea specimen, while maintaining an *in vivo* environment. The load and displacement are controlled through a data acquisition system. The chamber places a completely saturated environment and temperature is maintained at $37 \pm 1^{o}C$. The load provides an accuracy of ±0.01N and displacement of 1% of the specimen's length (80-200 μm).

The quartz glass did not arrive as scheduled however an alternate design using acrylic will be implanted to successfully complete the tasks of the project. Two tests will be preformed to display the success of the design. One test will consist of a dry environment with a non submersible load cell. A load will be applied to a rubber band to show the reaction from the load cell and the values of displacement. The second will test heating system by circulating the fluid through chamber. The non-submersible load cell will be replaced with a stainless rod. Once the submersible load cell is available the system will be fully automated

Ryan Cahill

Kelli Church

Brad Jaworski

Collagen Bioreactor

Design Team

Ryan Cahill, Kelli Church
Brad Jaworski

Design Advisor
Prof. Jeff Ruberti

Abstract

Tissue engineering promises to revolutionize treatment of connective tissue disease and injury. Tissue engineers can generate collagenous matrices but they are typically unable to bear *in vivo* loads. It has been shown that application of mechanical load to living collagenous matrics results in the improvement of mechanical properties and organization. The tissue is theroized to reorganize under tensile load in order to compensate for the force applied to it. Currently bioreactors capable of applying a mechanical load are being developed for large connective tissue however; nothing is developed for cornea or other small tissue specimens. Small tissue or cornea is highly organized and load bearing however there is no comparable device. The basis of our project is to design a miniature bioreactor capable of appying mechanical loads and resulting in organized cornea development. The cornea will be housed saturated enviroment at 37°C while controlling strain and load. The bioreactor must measure the force applied to ±0.01 N and the displacement to 1% of its overall lengh (0-200 µm). Cornea will be used in testing with dimensions of 2-4 mm length, by 8-20 mm length and only 50 microns thick. The specimen must be completely statuated in a sterile, anticorrosive visible environment at body temperature. A requirement was added later in the semester which included a 3 mm distance between specimen and outside enviroment. The requirement lead to a sliding quartz glass tubing design as seen in Figure 1. The quartz glass slides up to load specimen and is compressed down to seal container maintaining a 3 mm distance and a visible specimen. Copper block were used to heat chamber and pre heat tubing with the entering circulating fluid. Heat transfer analysis confirms the specimen will be heated to 37°C in 80 seconds. A zaber screw actuator was used to apply a force and measure displacement and a subermsible load cell was used to measure the amount of force applied. The following summary states the requirements needed, design and components selected, as well as thermal and mechanical analysis completed.

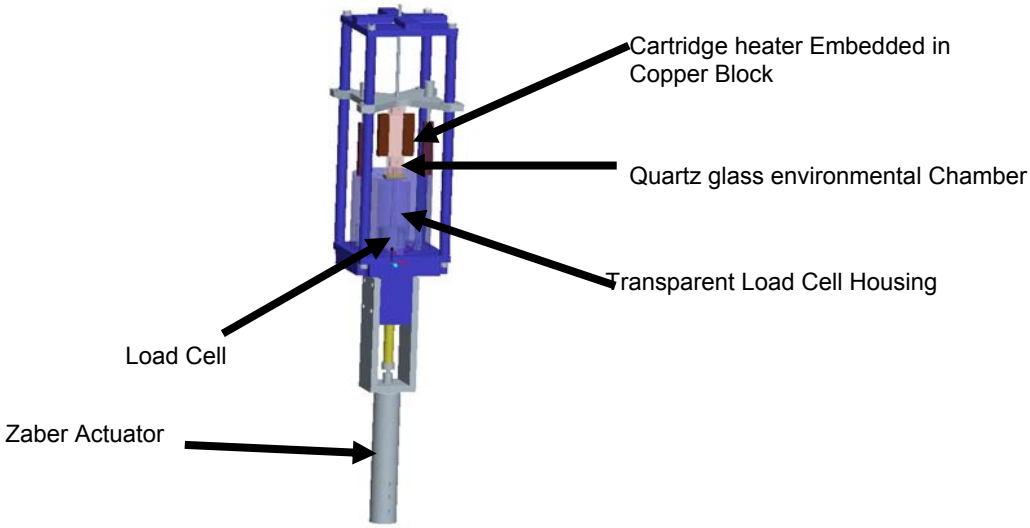

Figure 1: Collagen Bioreactor Final Design and Components

The purpose of the project is to create a successful bioreactor for soft tissue specimens which will adapt to an applied mechanical load.

The bioreactors for have been used in industry but load bearing bioreactors are only available for large connective tissue. There are none that have been created for the use of small collagenous tissue such as cornea. The main goal of this project is to successfully design a bioreactor capable of applying mechanical load to small tissue specimens. This new genre of bioreactors is used to apply loads to living collagenous tissue order to generate a stronger, more usable connective tissue. Collagen bioreactors apply mechanical load to a tissue specimen which produces a cellular response from the fibroblasts. It is theorized that the microstructure of living collagenous matrix will adapt to and align itself in the direction of an applied load.

The Design Project Objectives and Requirements

The device must precisely measure force (±0.01 N) and displacement (80-200 µm) of the specimen with high accuracy while being saturated in a sterile environment at body temperature. Specimen must be saturated and at body temperature throughout experimentation. All material touching saline solution must be autoclavable anticorrosive, and viewable. (Ref 3)

Design Objectives

The main project objective is to create a load bearing bioreactor for soft tissue specimen who can measure force and displacement. The force and displacement inputs shall be easily entered into the testing system mounted in a readily accessible location. The fixture shall be comprised of an accessible readout and control system. The device must be calibrated before each use to zero the displacement measurement device. The soft tissue must be gripped without slipping or damaging the specimen. The tissue must also be completely submersed in a saline solution throughout testing and remain at body temperature. To keep a homogeneous mixture of nutrients in the fluid, it must also be circulated throughout the chamber. The nutrient bath will be completely emptied and refilled with a clean solution when necessary. The device must maintain the sterile environment throughout test cycle. Any surface in contact with tissue and fluid must be anticorrosive. The tissue sample should be easily accessible to the user, and the specimen should be viewable.

Design Requirements

The tissue used for this project is cornea which is 8-20 mm in length, 2-4 mm in width and only 50 microns thick which places a high demand for precision with all calculations. The main requirements of the project include measuring the force within ±.01 N and displacement of a collagen specimen within 1% of its

length (80-200 μm). The tissue specimen must be kept in a sterile saline solution at 37 ^{o}C ±1°. In order to maintain the sterile environment the surfaces touching fluid and specimen must be able to withstand the temperature of the autoclave at 120°C. Later on in the semester a requirement was added consisting of a 3 mm distance between specimen and outer environment.

Design Concepts considered

The designs have evolved from a simple cantilever beam concept, electromagnetic force design, to a complex baseline design (ref 6).

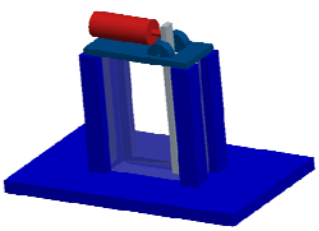

Figure 2: Cantilever Beam Design

The initial design was a lever arm design. A long vertical beam would have a pivot point near the top, while the bottom of the beam would have a clop pinned to it, giving two degrees of freedom and allow for the sample to be stretched in an arcing motion. Considering that the actuator would be applying a force to the uppermost part of the lever arm, and the ratio of distance from the pivot point to the force application was known we could multiply displacements as well as magnify the amount of force exerted by the actuator. However, after reviewing the requirements there were several drawbacks to the design including accuracy of force and displacement. While the displacement could be measured optically, it would not give the accuracy required. This is due to the fact that the lever arm would move in a radial motion, causing vertical and horizontal displacement. A more precise form of data acquisition would also be needed to sustain the ±0.01 N accuracy. (Ref 6.1)

A brief design was created implementing an electromagnetic force. The use of magnets and electrical current would eliminate the need for the moveable arm in the tank and would allow for only one degree of freedom. The moveable arm would be replaced with a magnet on the outside of a tank connected to a foam medium attached to the conducting metal attached to the grips with the tissue. When comparing the electromagnetic design to the requirements many aspects were investigated further and some adjustment would be made. Electromagnets would allow many advantages such as a completely enclosed volume, as well as a single degree of freedom motion, but since this type of technology is unreliable in a system such as this, a different force source was chosen. Also naturally buoyant grips were an idea in this situation but they are expensive and hard to find for the application needed. (Ref 6.2)

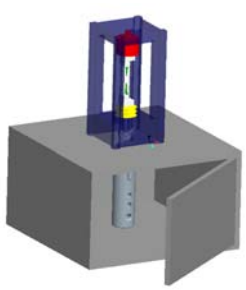

Figure 3: Original Baseline Design

Our initial baseline design was a two part system with the saline container holding specimen on top and a control box on bottom. The top part will consisted of specimen, grips, force transducer, and load cell. By moving the transducer to the inside of the test chamber the system can be designed to override the friction applied by the gasketing required to seal the chamber. All of the control system components will be mounted into the base pedestal and be protected from any potential leak damage. Through mounting the components inside a base frame, we will be able to construct a highly accessible display, as well as an aesthetic design. (Ref 6.3)

Recommended Design Concept

The design implements a quartz glass tube which can be slid up to insert specimen and be locked down to seal specimen inside. The quartz glass incorporates the new requirement of a 3 mm distance between specimen and outside environment. Copper block were placed outside chamber to heat fluid inside chamber as well as preheating the fluid entering the chamber through a silicone tube inside copper block.

The following section will describe the final sliding glass design, and the components selected, as well as the heat transfer analysis completed in order to confirm the system will be adequately heated. The key advantages to the recommended concept will also be summarized at bottom which includes the ability to preheat the fluid, sliding quartz glass for easily accessing specimen, and the ease of use with data acquisition system.

(1) Design Description

The initial baseline design had some changes made in order to accommodate a new requirement. The specimen is now required to be viewed on two sides with a 3 mm distance from specimen to outside environment. The housing for the specimen would now be configured in quartz glass tubing, which inner dimensions (7 X 13 mm) will withstand the new specifications. Also this new requirement limited the total volume of saline solution as well as the allowable working area. The rest of the design is the same as the initial baseline design. The bottom grip is attached to a long adapter and attached to the load cell. The actuator is located and attached underneath the load cell. (Ref 6.4)

The following section describes the components selected for the project. A linear actuator was required to apply a force while at the same time measuring the displacement. A Zaber screw actuator was implanted because it meant specification for displacement (ref 3), was low cost and software could be incorporated with Labview. A Honeywell sensotec submersible load cell was used in design because

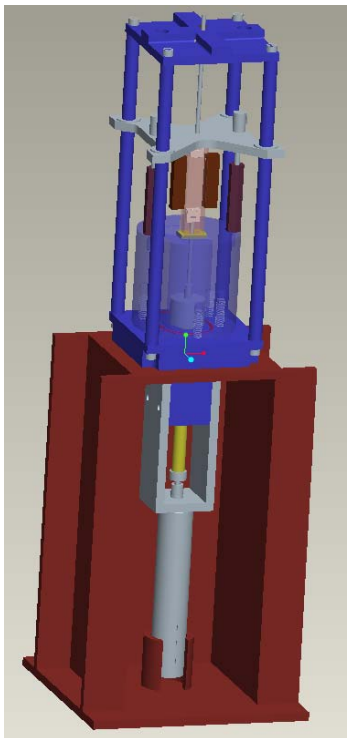

Figure 4: Sliding Glass Design

it was the only load cell which was submersible, and was capable of measuring force within ±0.01 N. Sealing the chamber is crucial to containing the nutrient bath, as well as keeping a sterile environment High temperature silicone rubber seals and gaskets will be embedded into the interface areas between the glass tube and the structure of the bioreactor to allow these sterile conditions and prevent leaks. The structure of the reactor is mostly polycarbonate which is transparent, anticorrosive and autoclavable. The fluid will be circulated through the chamber using a peristaltic pump. Cartridge heaters will be used to heat a copper block which distributes heat to the chamber. These two blocks will symmetrically be placed on either side of the chamber. Silicone tubing from the peristaltic pump will be placed through the copper block to preheat liquid to body temperature that is entering the chamber. Computer automation is necessary due to the extremely fine measurements and adjustments required. The labview program will interact with the hardware and create a dynamic control system, capable of responding to force changes in less than a second. (Ref 7)

(2) Analytical Investigations

The surfaces in contact with the environment will be composed out of medical grade 316L stainless steel. This will allow for minimal deflection because of the ratio of the moduli, and maintain a corrosion free environment. From ansys analysis, the 0.2 lbs does not produce a significant displacement in the frame. (Ref 8.1)

Heat transfer analysis was completed to the copper block and chamber to confirm that the specimen temperature could be maintained. Heat transfer analysis was also completed on silicone tubing and pre-heating saline from peristaltic pump. Both heat transfer analyses (heating liquid inside tank and pre-heating fluid) were incorporated into one analysis. The copper block would reach a high temperature of 50°C with 1/8” foam silicone insulation. At about 1 minute, chamber fluid will reach body temperature and will reach steady state at 80 sec. The preheated fluid will adequately reach body temperature by time it enters chamber at a velocity of 0.5 ml/min. The dimensions are 15 x 40 x 8 mm (Ref 8.2).

(3) Key Advantages of Recommended Concept

The main advantages of the final design are the sliding glass

tubing, preheating the fluid, and vertical design. The dimensions of quartz glass fulfill the requirements of a viewable specimen as well as maintaining 3 mm distance on two sides of the chamber. The unique side design of the glass allows for easily access to the specimen and the tight seal should minimize leakage. Also by using the outside heating block to pre heat the fluid entering, there is a minimal amount of heat difference entering the chamber, allowing for quicker steady state temperature. The overall design allows the user to place the chamber on its side as needed. This is important when using inverted microscopes to examine the specimen.

Financial Issues

The cost of the design is around $3,000 due to the submersible load cell, actuator and data acquisition system.

Bioreactors are a fairly new technology and are generally used for large connective tissue such as ligaments, tendons, and cartilage. There are none have been created for small tissue such as the cornea. There are however environmental chambers available to house and apply mechanical load to small tissue specimens. MTS and Instron have created devices with similar specifications. Water baths are mounted onto the machines to give in vivo environment for specimen. MTS and Instron machines are extremely precise and have a variety of mechanical analyses, however they cost above $50,000. Since the project is only used to measure force and displacement the cost will be around $3,000. The main cost of the bioreactor is the load cell ($800) , the actuator ($750) and the data acquisition ($1111)

Recommended Improvements

Eliminating the need to drill through the quartz glass.

The design required drilling the quartz so the preheated liquid enters at body temperature without being exposed to the open air. Quartz is an extremely hard material which created problems when drilling through it. A better solution would be to have the silicone tubing pass through the top or bottom and have the tubing incased in copper.

Table of Content

List of Tables

List of Figures

1. Acknowledgements

The Collagen Bioreactor group would like to give a special thanks to our advisors, Prof. Ruberti, and Prof. Kowalski, for their day to day support. Without their counsel and instruction the bioreactor would not be the fine example to engineering precision that it is today. Other Northeastern faculty member's that deserve thanks are, Kevin McCue and Richard Weston. Their advisement pointed us in the right direction and got our data acquisition system on its feet. Jeff Doughty with his flawless purchasing aid also deserves our appreciation. In the NU machine shop, Jon Doughty also provided us with priceless advice. Seeking help outside of the University for extensive machining capability, we were fortunate enough to have resource such as Raymond Laliberte and the Boston Scientific machine shop staff, a very special thanks goes out to them. Without the guide from these key people and their individual specialties, we would not have a successful device. Thank You.

2. Introduction

The bioreactors have been used in industry but load bearing bioreactors are only available for large connective tissue. There are none that have been created for the use of small collagenous tissue such as cornea. The main goal of this project is to successfully design a bioreactor capable of applying mechanical load to small tissue specimens. This new genre of bioreactors is used to apply loads to living collagenous tissue order to generate a stronger, more usable connective tissue. Collagen bioreactors apply mechanical load to a tissue specimen which produces a cellular response from the fibroblasts. It is theorized that the microstructure of living collagenous matrix will adapt to and align itself in the direction of an applied load. The main project objective is to create a load bearing bioreactor for soft tissue specimen who can measure force and displacement. The force and displacement inputs shall be easily entered into the testing system mounted in a readily accessible location. The fixture shall be comprised of an accessible readout and control system. The device must be calibrated before each use to zero the displacement measurement device. The soft tissue must be gripped without slipping or damaging the specimen. The tissue must also be completely submersed in a saline solution throughout testing and remain at body temperature. To keep a

homogeneous mixture of nutrients in the fluid, it must also be circulated throughout the chamber. The nutrient bath will be completely emptied and refilled with a clean solution when necessary. The device must maintain the sterile environment throughout test cycle. Any surface in contact with tissue and fluid must be anticorrosive. The tissue sample should be easily accessible to the user, and the specimen should be viewable

The tissue used for this project is cornea which is 8-20 mm in length, 2-4 mm in width and only 50 microns thick which places a high demand for precision with all calculations. The main requirements of the project include measuring the force within ±.01 N and displacement of a collagen specimen within 1% of its length (80-200 μm). The tissue specimen must be kept in a sterile saline solution at 37 ^{o}C ±1°. In order to maintain the sterile environment the surfaces touching fluid and specimen must be able to withstand the temperature of the autoclave at 120°C. Later on in the semester a requirement was added consisting of a 3 mm distance between specimen and outer environment.

The collagen bioreactor will be comprised of components that meet the requirements of the project. The major components of the project will be: actuator, load cell, heaters, heat controls, data acquisition and grips. Trade studies were completed on each element of the bioreactor system and the most suitable component was selected based on the results. Trade studies were not done for the load cell and the data acquisition system due to the specificity of the requirements and relatively small markets for each. Finally a comprehensive design was created around these components in order to house the specimen. Several designs were created over the span of the capstone class and guided through the many constraints and requirements.

3. Background

Collagen is the primary building block of load bearing tissue. Collagen is secreted from fibroblast cells and is comprised of long monomers with a unique triple helix shape. Fibroblast cells live in connective tissue, some examples are: ligaments, tendons, cartilage, and cornea. Fibroblasts secrete collagen as a response to stimuli, including mechanical load. Tissue engineers put fibroblast cells into collagen matrices in hopes the cell will grow. The purpose of the collagen bioreactor project is to use mechanical load to provoke a response from the fibroblast. The following section will explain the structure, function and process of collagen.

There are over 20 different types of collagen and types I, II, III, V, XI are all self assembling. Self assembling collagen rebuilds itself automatically with 80%-90% of collagen in the body being comprised of type I, II, and III. The collagen bioreactor group will be using Type I collagen to perform all experiments. In the body, Type I collagen is synthesized in response to injury. Gram for gram collagen is stronger than steel.

Collagen is formed from several long thin fibrils with an axial periodical structure. The fibrils provide the major biomechanical scaffold for cell attachment and anchorage of macromolecules, allowing the shape and form of tissues to be defined and maintained. Collagen fibrils are comprised collagen monomers. Collagen monomers have a unique triple helix shape containing 3 polypeptide chains. The triple helix is formed through gly-x-y, together create the polypeptide chains. Gly- stands for glycine which must be present to form the triple helix, because it is the only amino acid that can fit into the crowded center of the three stranded helix. The other x- and y- are amino acids, usually proline and hydroxyproline. Each chain contains precisely 1050 amino acids wound around one another in a characteristic right handed triple helix. The monomers within the fibrils-forming collagen fibrils are 300 nm of continuous triple helix followed by a 1.5 nm cross section globular section consisting of telopeptides representing 2% of overall length.

4. Requirements and Specifications

The following are a list of requirements for each aspect of design:

1. Mechanical Measurement Error
   - 1.1 Device shall measure the length of the specimen before, during, and after tensile testing.
   - 1.2 Measurement of the length of the specimen shall be held to within the given accuracy.
   - 1.3 Device shall be calibrated before each use to zero the displacement measurement device.
   - 1.4 Device shall measure the force applied to the specimen before, during, and after tensile testing.
   - 1.5 Measurement of the force applied to the specimen shall be held to within the given accuracy.
2. Sterilization
   - 2.1 Device shall maintain a sterile environment throughout a test cycle. Environment shall be sealed off and form an enclosed environment.
   - 2.2 Device shall be sterilized at the end of every cycle or when deemed necessary. Any surface in contact with tissue sample or its medium shall be sterilized in an autoclave at $120^{o}C$
3. Environment Variables
   - 3.1 Tissue shall be saturated in a nutrient medium through the duration of the test.
   - 3.2 Tissue medium shall maintain a constant temperature of $37^{o}C \pm 1^{o}C$.
     - 3.2.1 Nutrient Medium must be changed whenever necessary. Access ports shall be installed to allow changing of medium.
     - 3.2.2 Nutrient bath will be completely emptied and refilled with a clean solution.
4. Material Properties
   - 4.1 The device shall be comprised out of material that can withstand a corrosive environment as well as the temperature of an autoclave.
   - 4.2 The device shall be comprised out of material that can withstand the temperature of an autoclave.
5. Human Interfaces
   - 5.1 The Tissue sample will be easily accessible to the user. Doors and/or hatches will be installed for accessibility purposes.
   - 5.2 The fixture shall be comprised of an accessible readout and control system. The force and displacement inputs shall be easily entered into the testing system mounted in a readily accessible location

5. Marketing Research

Bioreactors are a fairly new technology and are generally used for large connective tissue such as ligaments, tendons, and cartilage. None have been created for small tissue such as the cornea. There are however environmental chambers available to house and apply mechanical load to small tissue specimens. MTS and Instron have created devices with similar specifications. MTS and Instron machines are extremely precise and have a variety of mechanical analyses, however they cost above $50,000. A modified Instron Machine, called the Biopulse is also in production (see figure 2. This device is similar to other products on the market, but this specific type has analytical features built into the set up. This machine is used for low force application, is submersible and supplies a sterile environment. A variety of high and low capacity grips are also available to clip the specimen depending on the tissue structure. MTS creates several biomaterial machines including 658 Mini-Bath™, see figure 3. The MTS system is viewable and can be used for small scale tissue, for example eye cornea tissue. MTS and Instron have very similar designs and applications for their device and cost above $50,000.

Figure 2: MTS 658 Mini Bath

Figure 3: Instron Biopulse Device

Tissue Regeneration Inc. (TRI) is partly owned by Tufts University is in preclinical trials for a new procedure that would allow the body to grow its own anterior cruciate ligament (ACL), a commonly injured knee ligament. (

Figure 4) Through the use of a bioreactor, mechanical load is applied to the cells along with collagen fiber which result in organized collagen based on the mechanotransduction of the collagen microstructure. The company is also branching off to create a bioreactor for cartilage, particularly rotator cuff cartilage. The tissue engineering being done at TRI is revolutionary to the field and is evidence of the use and need of bioreactors. While larger bioreactors for ligaments and tendons are up and coming in the field of tissue engineering, there is currently not a successful bioreactor for small tissue in the field.

Figure 4: TRI bioreactor for ACL

6. Design Layout

The bioreactor design has changed over the course of this semester. This is due to two main variables. First, the method and orientation of applying force to the tissue, and second is the physical components selected to perform the tasks. As one changes, usually so must the other. As seen below in the schematic diagram, various components such as actuator, transducer, temperature controller, heaters, grips, and seals will be needed to apply the load and maintain environmental temperatures. Active control and data acquisition systems such as computer software will also be needed in order for the process to be completed successfully.

Designing a frame will be relatively simple except in the areas of extremely high tolerances. In these areas, extreme care must be taken to ensure proper readings during operation and measurement. Any frictional forces applied to the transducer will result in a misreading and cause a failure of the system. For this reason, the load cell must be placed in the chamber affixed directly to the tissue.

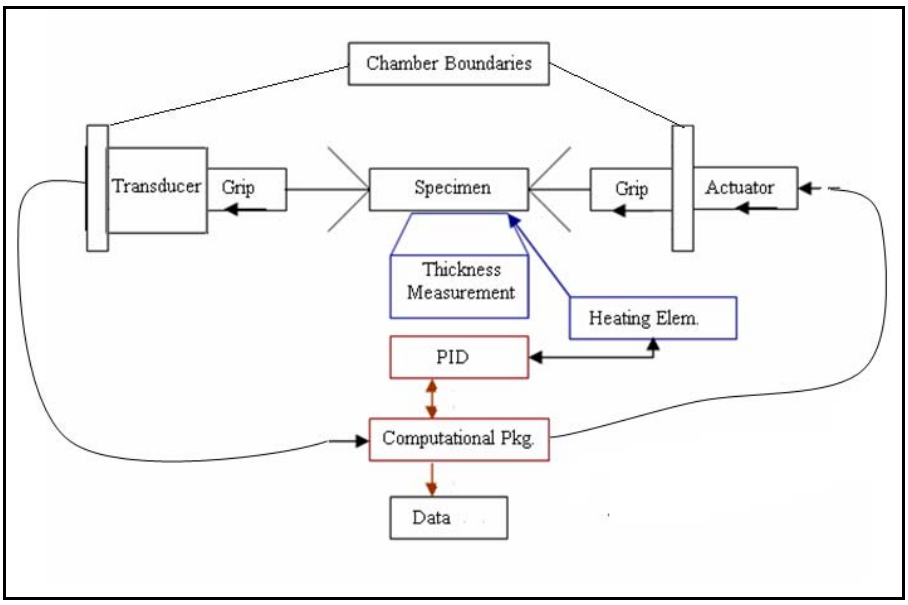

Figure 5: Layout of Bioreactor Operations

7. Design Evolution

Several designs have come out of brainstorming sessions, each one bringing the project closer to the final design concept. The design evolution is critical because through each revision, more of the requirements are taken into consideration and solutions to these requirements are formed in unison. Three major designs will be described and their benefits and drawbacks will be specified.

7.1. Lever Arm Design

The initial design was a lever arm design. A long vertical beam would have a pivot point near to the top. The bottom of the beam would have a clip pinned to it, giving two degrees of freedom and allow for the sample to be stretched in an arcing motion. The sample tissue would be placed between the grip connected to the beam and another grip on the opposing wall. A controlled force would be applied to the top of the beam using a linear actuator, and a resultant force would be applied to the sample via the pinned beam. (Figure 6: Cantilever Beam Design Concept) Considering that the actuator would be applying a force to the uppermost part of the lever arm, and the ratio of distances from the pivot point to the force application were known, we could multiply displacements as well as magnify the amount of force exerted by the actuator. The magnified displacement by the force could be measured by the use of an undetermined measuring device. The tank would be heated with the use of a water circulator and temperature would be controlled by thermocouples in combination with cartridge heaters.

The cantilever beam design was an inexpensive solution to the problem. After reviewing the requirements there were several drawbacks to the design including accuracy of force and displacement. While displacement could be measured optically it would not give the accuracy required. A calibrated ruler could measure the displacement to the nearest millimeter but an electrical system would limit human error when reading distance. Force applied to the lever by the actuator could be measured with the use of a spring, but were not limited to only the spring force. As the angle would increase the specimen would be pulled in the horizontal and vertical directions, causing problems in measurement of strain and force. The secondary force would be difficult to measure and accuracy would be limited. Calculations could be done to complete strain analysis, but with all the variables already within the system accuracy would be minimal. Since the

pivot arm involved a two-degree of freedom system and limited accuracy, a decision was made that all future revisions of this design must have one degree of freedom motion and all measurements must be aided by electrical system to have desired accuracy.

7.2. Electromagnetic Force Design

The use of magnets and electrical current would eliminate the need for the moveable arm in the tank and would allow for only one degree of freedom. It would be replaced with a magnet on outside of tank, connected to a foam medium attached to the conducting metal attached to grips with tissue. The force could be varied using a potentiometer to change the amount of current running to the magnet. A foam medium would be used as a spring to support the specimen, but must have a compressible length (has to stretch 4-20 mm) between the outside magnet and the inside metal. The magnet conductor would be suspended inside the tank by the use this foam medium. The load applied to the specimen would be applied through the force from the magnet to a metal

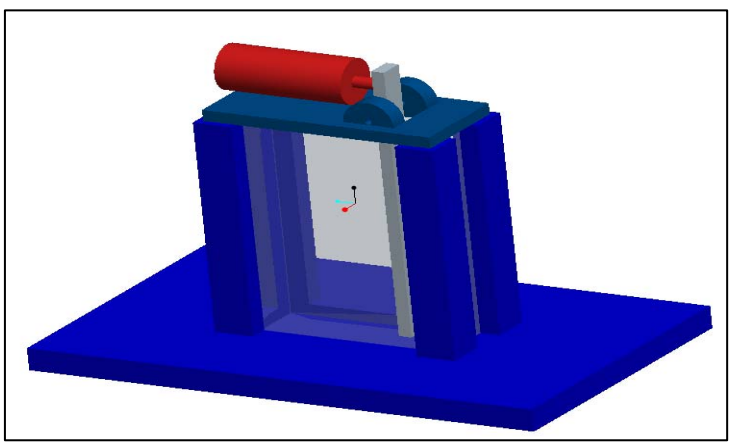

Figure 6: Cantilever Beam Design Concept

conductor (

Figure 7: Layout of Electromagnetic Design Concept). Measurement devices for strain had not been specified during this brainstorming idea, but force could be measured through magnetic force equations, or through a submersible load cell. The chamber would be a rectangular water bath made of plexi-glass in order to hold tissue. Since a water circulator is large, an alternate method would be used to heat water, such as

silicone heating pads with control box. To reduce the amount of solution being evaporated, small hollow plastic balls can be placed on top of the water to cover the bath.

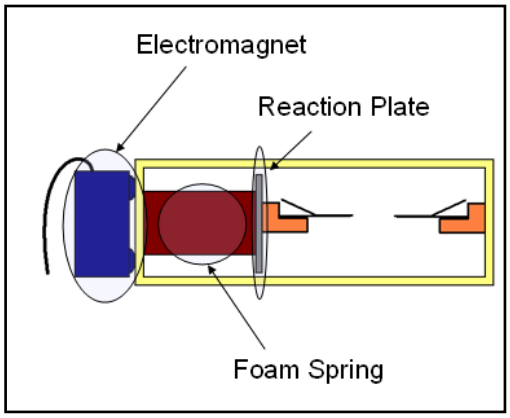

Figure 7: Layout of Electromagnetic Design Concept

When comparing the electromagnetic design to the requirements many aspects were investigated further and some adjustment would be made. The linear motion of the tensile force was limited variables and added control to the environment. The grips need to remain fixed in a one degree of freedom system to limit the effects of bending, therefore the system would need to stand vertical, or foam with the correct properties would need to be researched. Naturally buoyant grips were an idea in this situation but they are expensive and hard to find for the application needed. Strain would be measured with a data acquisition system, which has not been decided yet.

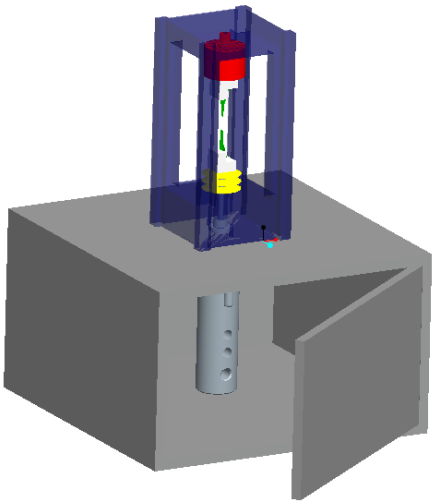

Figure 8: Initial Baseline Design

7.3. Design Three: Initial Baseline Design

In our previous baseline design, the tissue sample is placed in the test chamber. The test chamber would be constructed out of a high temperature plastic. The chamber is a two part system with the saline container with specimen on top and control box on bottom. The top part will consist of specimen grips force transducer and load cell. Moving the transducer to the inside of the test chamber, the system can be designed to override the friction applied by the gasketing required to seal the chamber. All of the control system components will be mounted into the base pedestal, and be protected from any potential leak damage. Through mounting the components inside a base frame, we will be able to construct a highly accessible display, as well as an aesthetic design.

The force is applied by the Zaber screw type linear actuator, through a boot bellows to provide a watertight seal. When the force is applied, the submersible transducer on the opposite end of the sample records the force applied, and sends the data to the computer. Based on the displacement and force recorded, adjustments will be made to the actuator to achieve a desired set point. A quartz glass window will be embedded into the chamber and sealed using an embedded o-ring seal. This chamber will be mounted on an aluminum base, which will contain all of the displays and control devices. This will also serve as a secure base for the linear actuator and test chamber.

The chamber can be orientated in two separate ways, either horizontal or vertical. Each orientation can be used to accomplish the goals needed in the project. Gravity is an obvious concern in the horizontal configuration. The sagging of the tissue and the moment created on the load cell by the grips could effect the system accuracy and performance. The most current design applies the vertical orientation to the chamber to eliminate the gravity factor, and measurement accuracy.

The flexibility of the materials used to construct the test chamber appears in the various specifications. Material used in the construction of the test chamber must be non-corrosive, transparent, and also must be able to withstand 120°C, the temperature of the autoclave. Chamber material is small in nature, but significant to the success of the design; therefore machinablitiy is a major factor. Metals are regularly used materials but are not desired for this project due to their corrosiveness. The next idea is a plastic material; it can be inert to the saline, machineable, strong, and possibly clear. Of the

plastics that we collectively have experience with and could suite our needs are: plexi-glass, Delrin, acrylic, and polycarbonate. Plexi-glass and other plastics were considered but do not have a high enough melting to withstand the high temperature during sterilization. Delrin is a very easy material to work with, it can withstand high temperatures, but it is not transparent. Acrylic is transparent, but it can be difficult to machine because it has the tendency to chip and it can crack with thermal and mechanical loads. Finally, polycarbonate seems to have all of the characteristics we want, and none of which we don't. Polycarbonate is translucent, inexpensive, can withstand high temperature, and meets specifications set by the Food and Drug Administration (FDA). Polycarbonate would not only provide a functional housing, it would also provide a very eye pleasing display.

Also, material must be selected to serve as a viewable port to the specimen. The glass portals will be used later to measure the thickness of the tissue over time. To accurately measure thickness the material for portals must be transparent, thus glass is desired. Quartz is the best option for clarity as well as withstanding temperature.

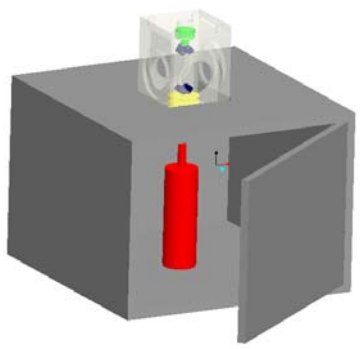

Figure 9: Bioreactor Assembly

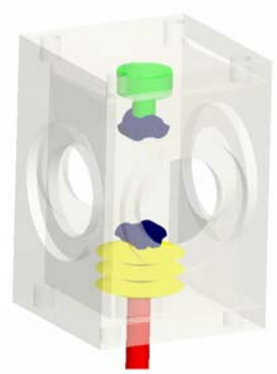

Figure 10: Bioreactor Test Chamber

7.4. Design Four: Final Design (modified baseline)

The initial baseline design had some changes made in order to accommodate a new requirement. The specimen was required to be viewed on two sides with a 3 mm distance from specimen to outside environment. The housing for the specimen would now be configured in quartz glass tubing, which inner dimensions (7 X 13 mm) will withstand the new specifications. Also this new requirement limited the total volume of saline solution as well as the allowable working area. The rest of the design is the same as the initial baseline design. The bottom grip is attached to a long adapter and attached to the load cell. The actuator is located and attached underneath the load cell

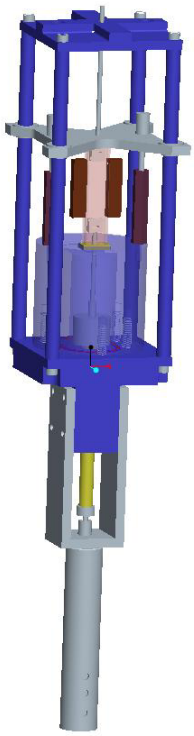

Figure 11: Final Chamber Design

A scaffolding was construted to reach around the specimen and support the upper area of the sample. This scaffolding will also serve as a sealing area as well as a storing area for the new quartz glass tube chamber. Because of these new changes, the overall height of the system grew from about 8 inches to around 16 inches, and the overall volume required to fill with fluid decreased dramatically. The superstructure of the bioreactor will be composed out of medical grade 316L stainless steel. This will allow for minimal deflection because of the ratio of the moduli, and a corrosion free

environment. As seen from the Ansys analysis, the .2lb load does not make the system as a whole displace a noticeable amount, thus reducing the error. All other systems used in the final design have been previously explained in the initial baseline design section of the report.

8. Selected Design Components

As mention in the Design Layout section, the following are the necessary components vital to the success of the system. Trade studies were completed to assess which product was the best for the needs of the project. Mechanical analysis was also completed when needed.

8.1. Linear Actuator

To apply the force to the specimen, a linear actuator was needed in order to be able to apply a force, while at the same time, measure the displacement down to 1% of the overall tissue length. The actuator we chose had to have a computer interface, a stroke length of at least 40mm, apply a .2N load, and have a step length small enough to allow a constant force function throughout the test. After considering other actuators in a trade study such as a LinMot and an actuator from Nook Industries, we decided to use a Screw Actuator from Zaber Technologies (Table 1). By using a Screw Actuator, we can take advantage of the digital readout, small component size, as well as the high accuracy of .1um. (Figure 12)

Figure 12: Zaber Linear Actuator

Table 1 : Linear Actuator Trade Study

Actuator	Weight	LinMot	Weighted Totals	Zaber Tech	Weighted Totals	Nook Ind.	Weighted Totals
Resolution	10	8	80	10	100	1	10
Interface	7	7	49	7	49	1	7
Max stroke	N ≥ 40mm = 0	-	0	-	0	-	0
Overall size	5	5	25	7	35	2	10
Price	7	7.6	60.8	8.4	67.2	10	72
			214.8		251.2		99

8.2. Force Transducer

To maintain high accuracy of force (within 0.01 N) the load cell must be submerged in the saline and attached to specimen. If load cell was placed outside the chamber, accuracy would be limited due to frictional forces from the various gasketing materials.

For the baseline model, a modified Sensotec model 31 will be used inside the chamber. The transducer will be made submersible by adding a sealant to the connection wires. This transducer can be purchased in a diverse range of forces, withstand the high temperature of sterilization, and is accurate to .15% - of full scale (approx .003N).

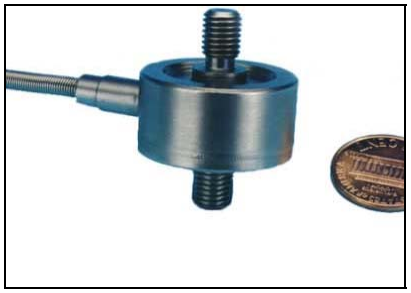

Figure 13: Honeywell Load Cell

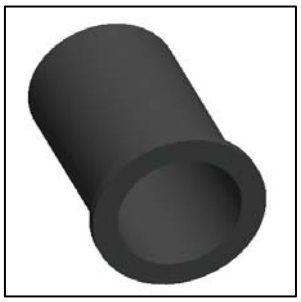

Figure14: Linear Bearing

8.3. Gripping Specimen

In the current baseline design, a single cam grip had been designed to transfer the load to the specimen, however later investigation lead to the dismissal of the cam grips and adhesive grips were implemented. This cam grip used a cam action roller to apply a normal load to the specimen which is proportional to the tensile load applied by the actuator. One potential problem was the size of the grip itself. In the new baseline design, the entirety of the grip needs to fit perfectly into the narrow test chamber. This feature limits the axial alignment into the chamber, and because of this, a linear bearing must be installed. The IGUS model HFM-1012-20. Even with the use of linear bearing, the single cams were removed and placed with thin rods with a flat side. The specimen is glued to posts and firmly secure. The posts take a much smaller amount of area inside tubing. The IGUS model HFM-1012-20. Along with alignment issues, this also causes the cam grip roller to have a 3mm diameter, which limits the gripping ability of the roller. The glue used which firmly hold specimen into place will be common medical grade glue with cynoacrylite.

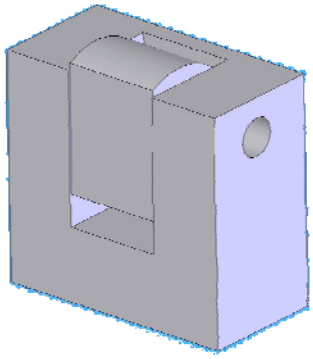

Figure 15: Single Cam Grips

8.4. Gasketing

Sealing the chamber is crucial to containing the nutrient bath as well as keeping a sterile environment. High temperature silicone rubber seals and gaskets will be embedded into the interface areas between the glass tube and the structure of the bioreactor to allow these sterile conditions and prevent leaks. Also the other components in the assembly must be protected from the fluid such as the linear actuator and sensing equipment.

8.5. Quartz Glass Tubing

The selected casing for the tissue specimen chamber is quartz glass based on its based on its material properties. Quartz Glass is utilized in the biomedical engineering field for its translucence because specimens are easily viewed. The material can be autoclaved at 120°C and is anticorrosive.

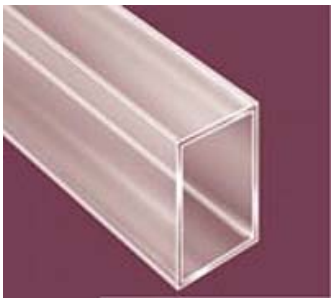

Figure 16: Quartz Glass Rectangular Tube

8.6. Fluid Circulation

Along with the temperature conditions, nutrient medium conditions must also be met in order to provide a clean and healthy living environment for the sample in question. Firstly the nutrient medium must be circulated throughout the chamber to keep the tissue sample healthy. Secondly, the medium must be completely changed out on a regular

basis (TBD). A peristaltic pump will be incorporated into this design to circulate the medium and keep a homogeneous solution throughout. The recirculation pump will then feed into the heating blocks, which will preheat the solution. From these blocks, an entrance in the quartz glass chamber will be created, and the solution will be entered directly from the side of the chamber. A valve will be placed in line with this recirculation pump, which will allow the system to be drained and refilled depending on the valve operation.

Figure 17: Peristaltic Pump

8.7. Temperature Controls

The requirements of the project call for physiological conditions, 37 degrees C ±1 degree. In order to maintain this condition we must implement a heating system containing heaters for the specimen and a temperature control box. The following sections discuss the heating element and temperature control box selected. Trade studies were completed to asses the best solution and mechanical analysis on heat transfer was completed.

8.7.1. Heating Element

While several heating elements were evaluated to meet the physiological and environmental restraints of the bioreactor design, the best solution was the cartridge heaters. Different types of heaters were considered for the application (cartridge heaters, silicone pads, rope heaters) and a trade study based on the requirements of the project was completed to select the best device. The trade study evaluated each selected heaters' ability to evenly displace heat quickly to the specimen at 37 ^{o} C ± 1° and meets the spatial

constraints of the design. Spatial constraints became very important because two sides of device must be translucent. The heaters surface area, power per unit area, ease of placement, uniform heat release and cost were the properties selected for trade study. Table 2 shows the properties selected as well as the weight of importance for project.

Table 2: Properties for Heating Element Trade Study

Property	*Weight*
Area	9
Power/Area (W/in^2)	7
Heater Placement	6
Cost	5
Uniform Heat Release to Specimen	5

Two different types of cartridge heater and silicone pads were selected to evaluate, one from Watlow and the other from OMEGA. Watlow and OMEGA both made cartridge heaters and silicone pads that could be used for the design but varied in price, style and power. Both cartridge heaters were anti corrosive and had the ability to be autoclaved but the OMEGA cartridge was a quarter-inch smaller and cheaper. However the Watlow Cartridge heater was capable of displacing heat throughout the cartridge, unlike the OMEGA which dissipated heat through the bottom. Also the Watlow cartridge could have different mountings put on the end of the cartridge such as a flange or thread. Silicone Pads were also selected from OMEGA and Watlow, however Watlow's product was far superior. OMEGA had silicone pads that fit requirement of product and are very cost effective but the Watlow product could be autoclavable and is extremely thin. A trade study was performed to give us a clear evaluation of the best solution.

Table 3: Results for Heating Element Trade Study

Property	*Device*			
	Cartridge Heaters OMEGA	Cartridge Heaters WATLOW	Silicone Pads OMEGA	Kapton Material WATLOW
Area	7	9	6	8
Power/ Area (W/in^2)	3	10	5	8
Heater Placement	9	9	8	8
Uniform Heat Release to Specimen	6	8	9	9

Cost	7.2	3	6.08	2
Weighted Results	**204**	**260**	**212.4**	**226**

The Watlow cartridge heater was selected from the trade study as the best solution. The cartridge heaters were better for placement because they could be placed within the chamber unlike the silicone pads which had to be placed on the outside. Through heat convection the heat could reach the specimen faster inside the chamber than outside. The heaters are also required not to take up much space because there must be a translucent view from at least 2 side of the device. Silicone heaters were superior in this respect because they could be custom made with holes for view points. Even though the Watlow cartridge heater was at a higher cost, but its ability to heat the element quickly and ease of use made it the best selection. The results of the trade study can be seen in Table 3. The complete trade study can be found in the appendices.

Figure 18: Cartridge heater

8.7.2. Temperature Controls

To control the heaters we chose to rely on the cost effectiveness and *ease of use* of an external temperature controller. Temperature controllers come in many different varieties and prices. First in the range of controllers are the On/Off types. These controllers simply toggle full power to the heaters based on the temperature input. Second are Proportional controllers. These controllers evaluate the difference between the set point temperature and the actual temperature and vary the magnitude of power to the heaters in an on/off fashion. Finally, there are PID (proportional, integral, and derivative) controllers. These allow the best control for small mass systems like ours. Along with proportional control, the integral and derivative controls analyze the amount of set point offset variance over time, and evaluate this rate of change to the heaters. This method is the most expensive, but its ability to limit temperature overshoot and react automatically

to small changes in the system, speak for itself. Other features we wanted the controller to have are listed in the trade study, located in the appendices.

The current design we are considering for maintaining temperature is using two cartridge heaters imbedded in conductive copper blocks fixed on two opposite sides of the chamber. To prevent temperature overshoot, the thermocouple will be located in close proximity to one of the heaters. This is especially a concern because we are using dense metals to transmit the heat. Overshoot occurs when the thermocouple is placed far from the heat source. What happens is that the controller registers a cold input from the thermocouple while the heaters ramps to full power. When the heat eventually reaches the thermocouple, the area around the heaters is much hotter than the desired temperature. Now as heat transfer continues, all areas will also exceed the desired temperature.

8.8. Data Acquisition Controls

System control is a very important aspect of our project. Automatic computer aid is a necessity due to the extremely fine measurements and adjustments required. The most critical of these adjustments is the force/strain relationship. The requirements call for the system to be force driven. This means that a set point force must be inputted, and whatever changes the specimen goes through (elongation, breakdown, etc.), this force must be maintained regardless of strain. This is similar to the temperature control process. Our ability to control the force became a conflict when we began searching for actuators. All of the actuators that we were looking at had software programs but they were all based on driving the actuator by position, not force. This forces us to look past the OEM software to custom software. A custom program would have to interpret the input from a force transducer and output the appropriate signal to the linear actuator. To answer this dilemma, we used LabView software to perform the necessary computational analysis, and input the signals via a signal connector block (BNC or screw terminal) to a digital I/O PC board. The LabView program will interact with the hardware and create a dynamic control system, being able to respond to force changes in less than a second. Along with the system controllability, the software will be able to take active data acquisition, recording the measurements and system status with time.

The program to provide a constant force was constructed in three "frames." The first frame was a modified manufacturer positioning program. The main block of code was kept in tact, while some of the variables were solidified. Once activated, this frame will return the system to its home position, and the operator must complete this step to move to the next, which is the specimen loading program. This next frame assumes that the specimen will be between 4mm and 20mm, and allows the user to input this data. When this is entered, the actuator extends, allowing for the user to insert the specimen in the grips. The third frame, is the main frame of this program.

The third program uses a fake DC circuit to cause a square wave, triggering the program into a sequence of TRUE/FALSE statements, which in turn, tell the actuator to either move or send back data. This feature was implemented due to the actuator's limit of 100 cycles per second. Anything over this rate would cause the motor to send back data at the same time as reading inputs, therefore crashing the program, and not allowing

the actuator to analyze its commands. Through this square wave frequency, the user can customize how often the specimen length should be checked, as well as how often the force should be increased/decreased. Through this TRUE/FALSE loop, the software can relay messages to and from the motor, causing a very high accuracy in reading the load as well as moving it in small increments, to be specified by the user. Every loop, the program checks the load cell voltage, and compares it with another user input. Depending if the voltage received is too high or low, the software tells the actuator to push or pull, respectively. Though this series of loops and commands, the actuator/load cell system works accurately and flawlessly.

8.9. Material Selection

The materials used in the superstructure bring out some questions regarding accuracy when measuring the strain of the specimen. If we were to use a material with a low enough modulus of elasticity, the .2lb force would deflect the plate reacting the specimen load. This problem was taken into consideration and found not to be a problem when using stainless steel as a frame. (Figure 19) With a displacement of approx $.484 \times 10^{-6}$ inches, the error will be negligible. This same condition is applicable about the rest of the superstructure.

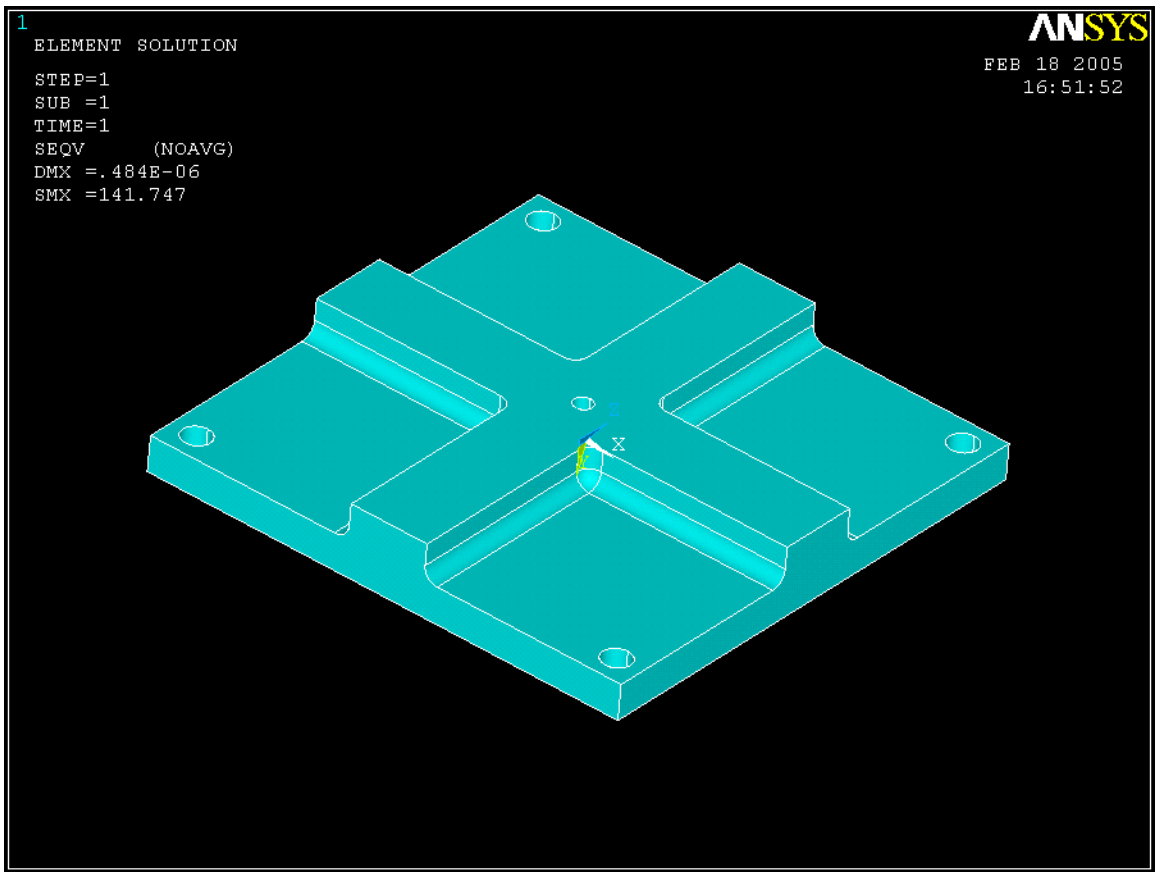

Figure 19 : Deflection of Upper Support Plate

8.10. Heat Transfer Analysis

Heat transfer analysis was completed to confirm the ability of the copper to adequately heat specimen within chamber and completely preheat fluid entering chamber to 37°C. The time needed to reach steady state body temperature was about 80 sec and the fluid was thoroughly preheated by time

it entered chamber. The velocity of the fluid through tubing was optimized to be 0.1 ml/min. Finite difference method was used along with nodal analysis to verify that the specimen is heated to body temperature. Only the glass, tubing, and liquid within the height of the copper were included in analysis.

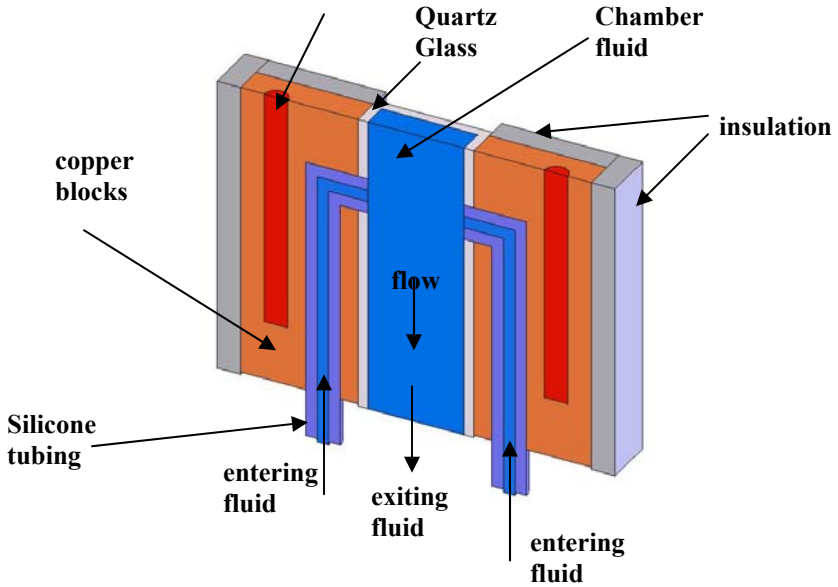

Figure 20:Heat Transfer Components and direction of Flow

The heating system is symmetrical; therefore analysis will be completed on only one side. Figure 1 displays the location of components, as well as the flow of the fluid. The fluid is pumped up the silicone tubing through quartz glass and enters chamber and exits through the base (which is not shown). The heat initiates at the cartridge heaters and dissipates through the copper block and glass into the chamber. The analysis consists of transient conduction and convection through solids and liquids as well as a parabolic flow in chamber.

Figure 21 is an overview of the system with the nodal volume divisions illustrated; this node system forms the basis of the numerical method. The last 5 nodes are tubing fluid nodes. The nodes are equally spaced between each material, and each node is consists of only one type of material. Finite difference analysis was preformed on each node. The finite dimensions were determined through analysis. Figure 22 expresses the equivalent circuit analysis for node 1. The analysis from the equivalent circuit consists of transient conduction and convection through solids and liquids as well as a parabolic flow in chamber.

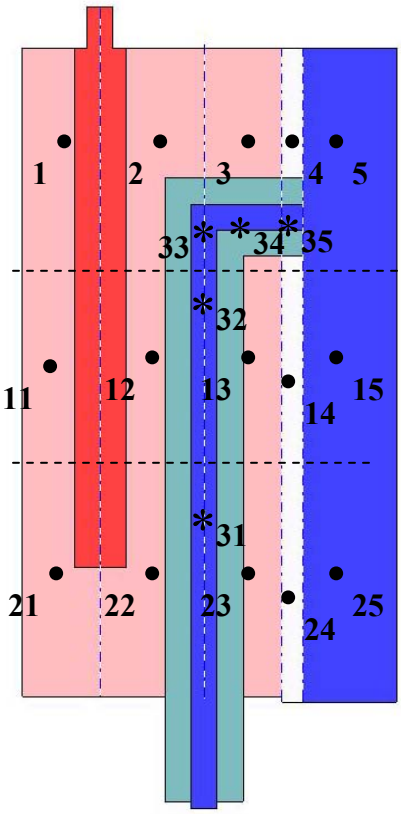

Figure 22: Nodal Analysis of Heater System

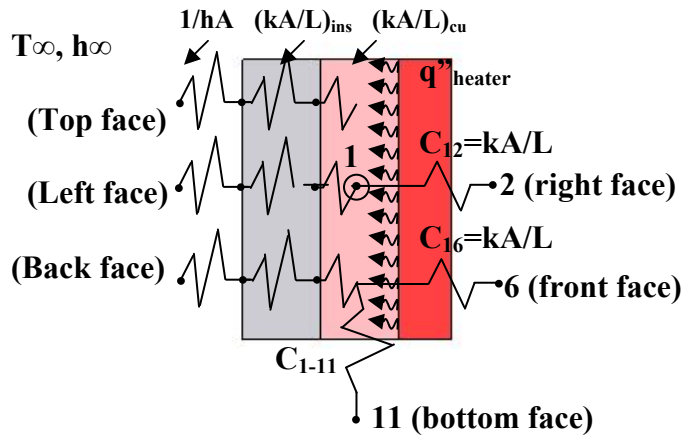

Figure 21: Equivalent Circuit Analysis for Node 1.

Energy balance was completed on all to estimate the chamber temperature after each time step. The following is an example of the energy balance results for node.

$$E_{in} = E_{out} + E_{stored}$$

$$q_{in} = q_{out} + q_{stored}$$

$$(\rho c V)_{cu} \cdot \frac{dT}{\Delta t} = \Sigma C_{ij} \cdot (T_{ji}) + (q'' \cdot A)$$

dT/dt simplifies to ΔT/Δt
q_{stored}= to amount of heat loss from heater

$$(\rho c V)_{cu} \cdot \frac{\Delta T}{\Delta t} = \Sigma C_{ij} \cdot (T_{ji}) + (q'' \cdot A)$$

$$\Delta T = \frac{\Delta t}{(\rho c V)_{cu}} \cdot [\Sigma C_{ij} \cdot (T_{ji}) + (q'' \cdot A)]$$

ΔT is equivalent to change in temperature over time $T_{final} - T_{inital} = T_f - T_i$

$$T_f - T_i = \frac{\Delta t}{(\rho c V)_{cu}} \cdot [\Sigma C_{ij} \cdot (T_{ji}) + (q'' \cdot A)]$$

$$T_f = T_i + \frac{\Delta t}{(\rho c V)_{cu}} \cdot [\Sigma C_{ij} \cdot (T_{ji}) + (q'' \cdot A)]$$

expand $\Sigma C_{ij} \cdot (T_{ji})$

The below equation is the final equation results for finding the final temperature. This is incorporated in the conductance formula for each face of finite difference block.

$$T_f = T_1 + \underline{\Delta t}\cdot[\, kA/\Delta x\cdot(T_2-T_1) + kA/\Delta y\cdot(T_6-T_1) + kA/\Delta z\cdot(T_{11}-T_1) + (1/(hA)_{air} + (kA/L)_{ins} + (kA/L)_{cu})^{-1}(T_\infty-T_1)]$$

The time step was evaluated by an increase in temperature. In order to find an accurate time step there must be a positive change in temperature. If the temperature change is too large the resulting temperature will oscillate. The following set of formulas was used to find time step.

$$0 < T_1\cdot(1 - \Delta t/(\rho cV)\cdot \Sigma C_{ij})$$

$$0 < 1 - \Delta t/(\rho cV)\cdot\Sigma C_{ij}$$

$$\Delta t/(\rho cV)\cdot \Sigma C_{ij} < 1$$

$$\Delta t < \rho cV/\Sigma C_{ij}$$

$$\Delta t < 0.8942\ J\cdot K / (2.5153+4.4473+0.556+2*7.96(10)^{-6}+9.956(10)^{-6})\ W\cdot K$$

$$\Delta t < 1.7\ s$$

$$\Delta t = 0.005s <<<<< 1.7s$$

The process was repeated for each node in the system. The lowest result for the time step was through the quartz glass which resulted in a time step of 0.005s.

The system also preheated the fluid entering the chamber through the copper block. Each node for the preheating fluid was incorporated into the heater system analysis. For the chamber fluid and the preheated tubing fluid, there is an enthalpic heat from the flow of liquid, which consists of the difference between the time step and mass flow rate multiplied by the temperature change. The temperature change is a result of the difference in the average temperature entering and exiting each node. The average temperature entering and exiting the nodes was calculated and then the overall change in enthalpy is found. The following is how the enthalpic equation was derived.

$$q_{out} = (\rho c)_l v_e A_f\cdot(T_{i+1}+T_i)/2 \longleftarrow \textbf{average flow exiting}$$

$$q_{in} = (\rho c)_l v_e A_f\cdot(T_{i-1}+T_i)/2 \longleftarrow \textbf{average flow entering}$$

$$q_{enthalpy} = q_{out} - q_{in} \longleftarrow \textbf{total enthalpy}$$

$$q_{enthalpy} = (\rho c)_l v_e A_f\cdot(T_{i+1}+T_i)/2 - (\rho c)_l v_e A_f\cdot(T_{i-1}+T_i)/2$$

$$q_{enthalpy} = (\rho c)_l v_e A_f/2\cdot(T_{i+1}+T_i-T_{i-1}-T_i)$$

$$q_{enthalpy} = (\rho c)_l v_e A_f/2\cdot(T_{i+1}-T_{i-1})$$

$$q_{enthalpy} = (\rho c)_l v_e A_f/2\cdot(T_{32}-T_\infty) \longleftarrow \textbf{fluid is entering from room temperature and exiting to node 32}$$

This calculation was then incorporated into the energy balance for each node having a flow. The following is the energy balance for the entering preheating fluid.

$$E_{in} = E_{out} + E_{stored}$$

$q_{in} = q_{out} + q_{stored}$, $q = q_{cond} + q_{enthalpy}$

$(q_{cond} + q_{enthalpy})_{in} = (q_{cond} + q_{enthalpy})_{out} + \cancel{q_{stored}}$ ← **no energy is stored, total enthalpy is in eqn. above**

$(q_{cond})_{in} = (q_{cond})_{out} + q_{enthalpy}$

$(\rho c)_l v_e A_f dT/dt = q_{31\text{-}32} + q_{31\text{-}cu} + q_{enthalpy}$ ← **Dt/dt is equal to ΔT/Δt**

$(\rho c)_l v_e A_f \, \Delta T/\Delta t = q_{31\text{-}32} + q_{31\text{-}cu} + q_{enthalpy}$

$\Delta T = \Delta t/(\rho c)_l v_e A_f \cdot (q_{31\text{-}32} + q_{31\text{-}cu} + q_{enthalpy})$ ← **ΔT is equal to temperature at final minus temp.initial**

$T_f - T_i = \Delta t/(\rho c)_l v_e A_f \cdot (q_{31\text{-}32} + q_{31\text{-}cu} + q_{enthalpy})$ ← **T_i is equal to T_{31}**

$T_f = T_{31} + \Delta t/(\rho c)_l v_e A_f \cdot (q_{31\text{-}32} + q_{31\text{-}cu} + q_{enthalpy})$

The resulting enthalpic and conduction calculations were added to energy balance. Below is the results of the energy balance.

$$T_f = T_{31} + \Delta t/(\rho c)_l v_e A_f \cdot (C_{31\text{-}32} \cdot (T_{32} - T_{31}) + ((1/(h_l \cdot A_f) + 2\pi r_o k_{si}/\ln(r_o/r_i) + 2\pi r_{cu} k_{cu}/\ln(r_{cu}/r_o))^{-1} \cdot (T_{22} + T_{23} + T_{27} + T_{28} - 4 \cdot T_{31}) + (\rho c)_l v_e A_f/2 \cdot (T_{32} - T_\infty))$$

The thermocouple was placed on the tubing just as the fluid as entering into the chamber. The velocity of the fluid was placed at slowest and the heater was placed on the highest allowable heat. The results display the heat will reach specimen and attain a steady state of 37oC in about 80 s, see graph below.

Table 4: Heating System Temperature vs. Time

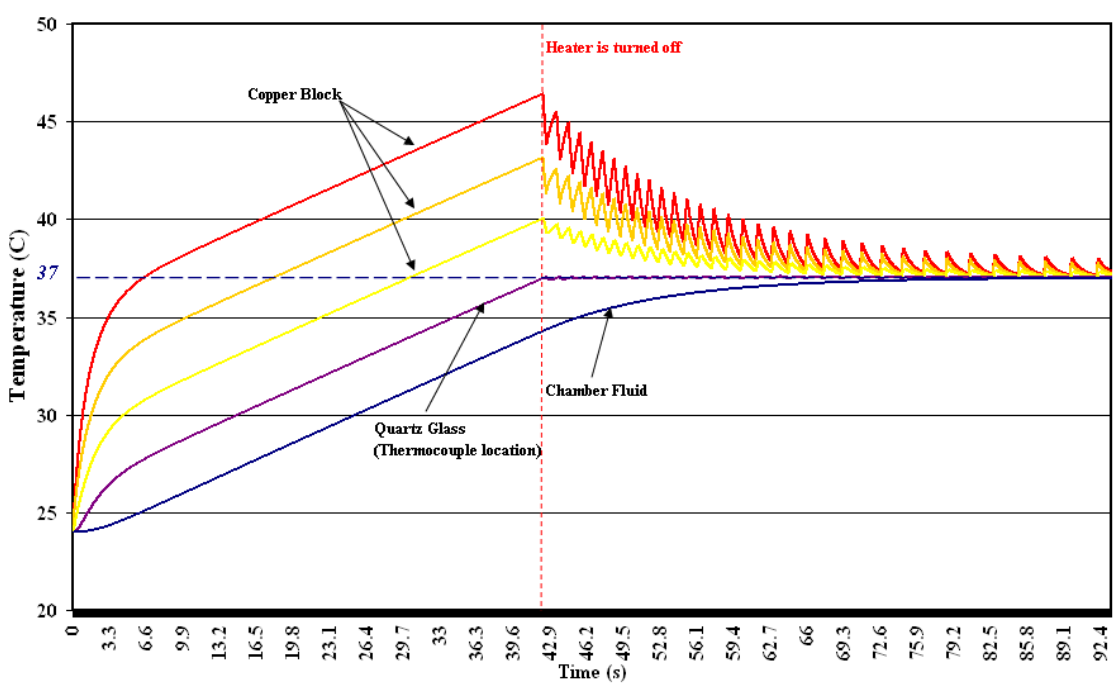

The graph displays the temperature for the top row of node, the results are typical for all three rows of system. The top three lines are the temperature results from the copper block. The highest temperature results are from the copper closest to the heater the following two are in order from the heater. The glass is represent in purple line and the thermocouple is located next at the load. The blue line represents the fluid inside the tank. A switch was implemented to represent a control system. Although a PID was used for the system the switch is a feasible to create in excel and represents a worse case scenario. The fluctuations in the graph are when the heater is disengaged is cause by the fluctuation from heat being absorbed and released. It can be concluded the temperature will reach equilibrium at about 80 sec.

The Table below displays the temperature in the chamber. Each line is a nodal section of chamber. The temperature change is about equal for each section. The temperature reaches body temperature within 80 seconds, and remains at steady state.

Table 5: Chamber fluid Temperature vs Time

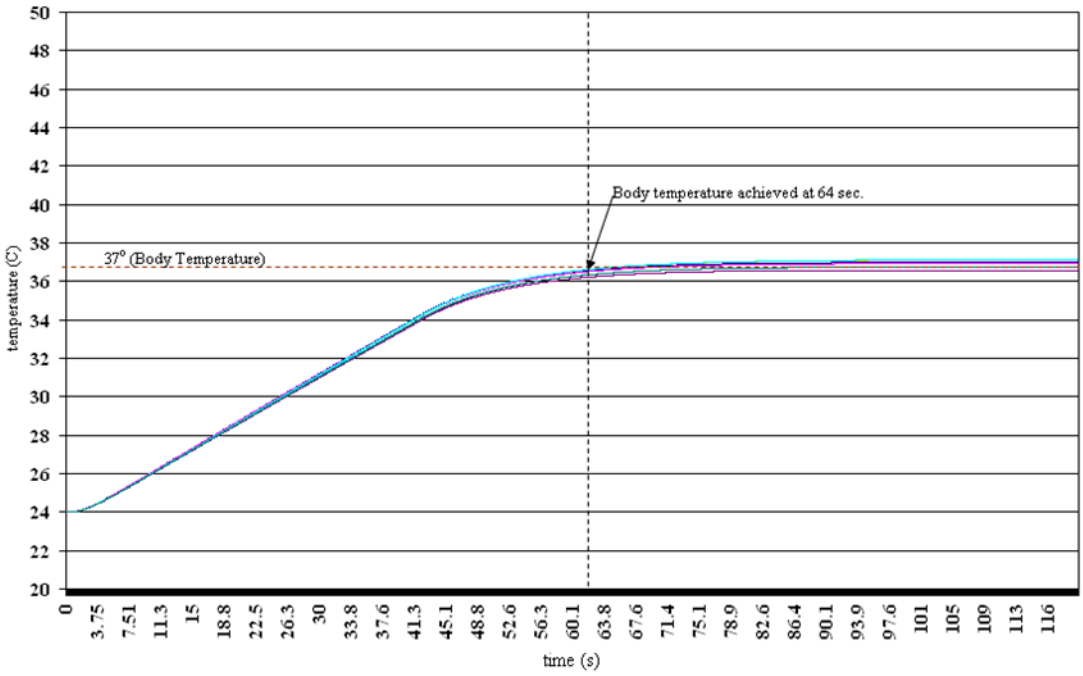

The final graph displays the temperature of the tubing as it enters the copper block and exits into the chamber. The temperature changes as it moves through the tubing into the glass and through the chamber but it reaches body temperature within 60 seconds.

The length of tubing was significant and the velocity is to be kept at lowest speed based on the analysis.

Table 6: Preheated Fluid Temperature vs Time

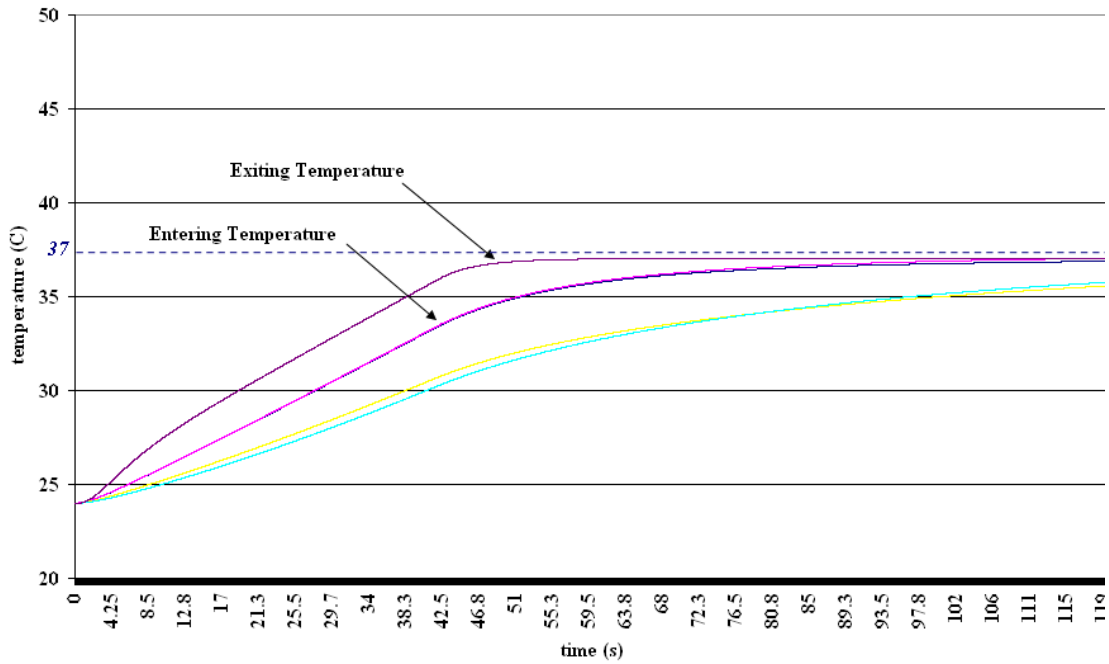

9. Experimental Analysis

The submersible load cell will not be delivered until after the semester is over to prove the device two experiments will be implemented with a non submersible load. The first experiment will verify the device will measure strain and force can be adjusted accurately. The second experiment will analyze if the system will be heated accurately and within range. During the first analysis the tank will be emptied a dry test will begin with non submersible load cell attached. The non submersible load cell will be removed for the second experiment, and replaced with a stainless steel rod. Load will not be read but liquid will pass through and temperature system will be activated.

10. Benefits of Design

The main advantages of the final design are the sliding glass tubing, preheating the fluid, and vertical design. The dimensions of quartz glass fulfill the requirements of a viewable specimen as well as maintaining 3 mm distance on two sides of the chamber. The unique side design of the glass allows for easily access to the specimen and the tight seal should minimize leakage. Also by using the outside heating block to pre heat the fluid entering, there is a minimal amount of heat difference entering the chamber, allowing for quicker steady state temperature. The overall design allows the user to place the chamber on its side as needed. This is important when using inverted microscopes to examine the specimen.

11. Drawbacks to the Design

The design isolates the load cell to a restricted environment. The load cell is located within the polycarbonate base and cannot be easily accessed. In order to access the load cell the device must be pulled apart. However, once in progress with testing the load cell should not have to be approached, only between testing. In order to have the load cell easily retrieved a gateway would need to be installed. However any kind of access point would create a possible leak point. Also the actuator is located underneath load cell and could be damaged during any outflow of water. Therefore it is a better interest to secure load cell inside and avoid leakage than have the load cell easily accessible and risk damage to the actuator

The design required drilling the quartz so the preheated liquid enters at body temperature without being exposed to the open air. Quartz is an extremely hard material which created problems when drilling through it. A better solution would be to have the silicone tubing pass through the top or bottom and have the tubing incased in copper.

12. Conclusion

Throughout the design of this project, there were many mechanical and environmental considerations that were taken in order to support the mechanotransduction of the collagen that is under examination. With each requirement, the system as a whole had to become smaller in order to compensate for the different viewing distances, volume requirements, and load applications. Various designs have

been deliberated in the process of added requirements and constraints. A simple cantilever design evolved into a complex two part chamber. The final design consisted of a top closed saline filled top with only 3 mm between the tissue specimen and the outside environment. Scaffolding was constructed to reach around the specimen and support upper area of the sample.

Based on the project requirements, the products were selected for each component needed for the design including: actuator, load cell, temperature controls, gaskets, fluid circulation, system control, and data acquisition. Trade studies were done to evaluate several products of each component to give the best solution for our project. To control the amount of force the Honeywell Load cell is implement because it is both submersible and can measure force to 0.01 N, meeting the design requirements. The Zaber actuator was selected in order to meet the accuracy requirement of 1% of overall length. The heating elements and thermocouples were modified in order to fit the smaller size and still maintain a stable temperature control. A VWR peristaltic pump was also added into the system due to an added requirement of fluid circulation in the chamber and throughout the system, and because of the size of the chamber, a preheating system was also added. In the final design, a very small, efficient, and cost effective system was formed. Custom Grips are being made to hold the specimen without causing damage to the tissue.

In the final presentation our design will be fully automated and assembled, and a test will be run to prove success of the device. The design will allow for in vitro testing of collagen and give the ability to apply a load to that specimen, and collect valuable data on load and displacement. The success of the project will add another application to the biomedical industry for the enhancement of soft tissue engineering.

Appendix A: Trade Studies

Linear Actuator

Actuator	Weight	LinMot	Weighted Totals	Zaber Tech	Weighted Totals	Nook Ind.	Weighted Totals
Resolution	10	8	80	10	100	1	10
Interface	7	7	49	7	49	1	7
Max stroke	N ≥ 40mm = 0	-	0	-	0	-	0
Overall size	5	5	25	7	35	2	10
Price	7	7.6	60.8	8.4	67.2	10	72
			214.8		**251.2**		**99**

Heater Selection

Property	*Device*			
	Cartridge Heaters OMEGA	Cartridge Heaters WATLOW	Silicone Pads OMEGA	Kapton Material WATLOW
Area	7	9	6	8
Power/ Area (W/in^2)	3	10	5	8
Heater Placement	9	9	8	8
Uniform Heat Release to Specimen	6	8	9	9
Cost	7.2	3	6.08	2
Weighted Results	**32.2**	**39**	**34.08**	**35**

Heater Trade Study Weighing Factors

Property	*Weight*
Area	9
Power/Area (W/in^2)	7
Heater Placement	6
Cost	5
Uniform Heat Release to Specimen	5

Heat Controller Selection

		Omega		Omron	
Feature	**Weight**	**Cni 3222**	**Cni 3223-C24**	**E5CS**	**E5CS-X**
Temp Stability	10	9	9	7	9
Accuracy	7	10	10	6	8
Universal Input	5	10	10	5	5
PC Interface	3	0	5	0	0
Autotue PID	7	10	10	6	10
2 Outputs	8	5	5	0	0
ramp to set point	5	5	5	5	5
Free Software	3	0	5	0	0
Price	8	9	7	9	8
TOTAL		**417**	**431**	**276**	**330**

Specimen Grip Selection

	Weight	ASSI arterial clamp	ASSI Weighted	Dillon Quatrol Double Cam Grips	Dillon Quatrol Weighted
Area (mmxmm)	9	0.04	9.98	496	2.00
Friction Force	8	9	9	9	9
Material Prop.	6	10	10	8	8
Attachment to load cell	8	5	5	5	5
Cost ($)	5	80	7.33	210	3.00
			41.32		**27.00**

Custom Double Cam Grips	Double Cam Weighted	Dillon Quatrol Pin Vice Grips	Dillon Quatrol Weighted
8X	9.0	546	1.0
9	9	6	6
8	8	7	7
10	10	9	9
20	9.33	145	5.17
	45.33		**28.17**

Appendix B: **Equations for Heat Transfer:**

Heat Transfer Analysis

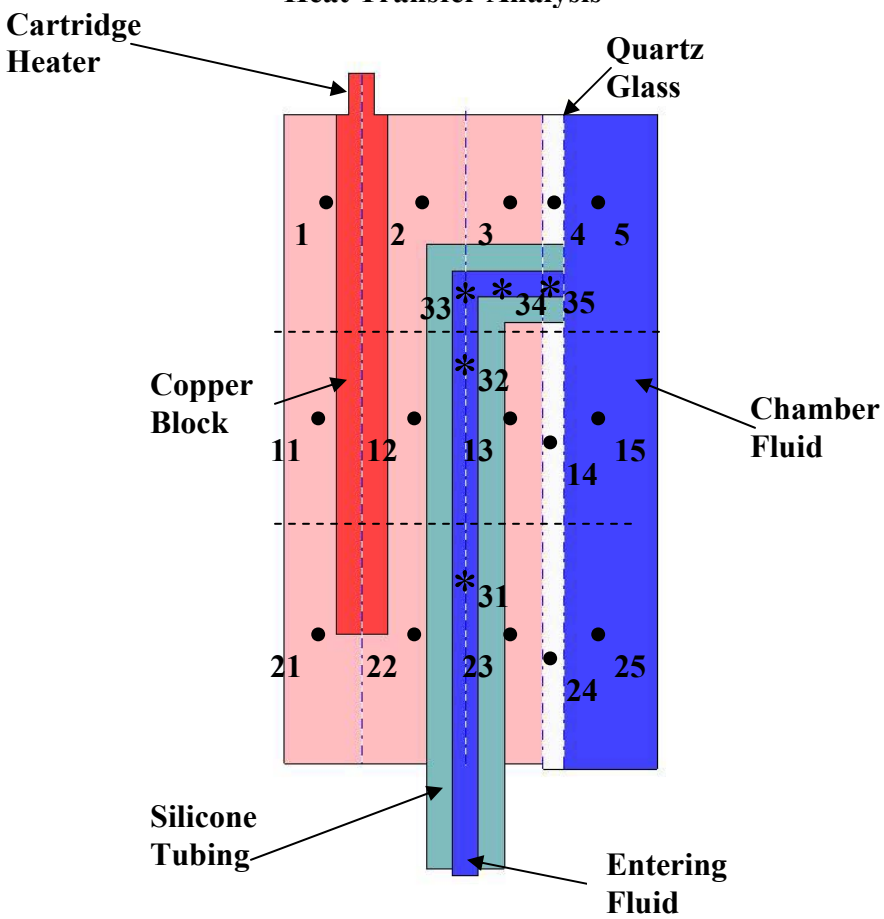

Figure 23: Nodal Placement of Heater Analysis (.=solid node, *=fluid node)

3-D Finite Difference of Solid and Fluid Nodes

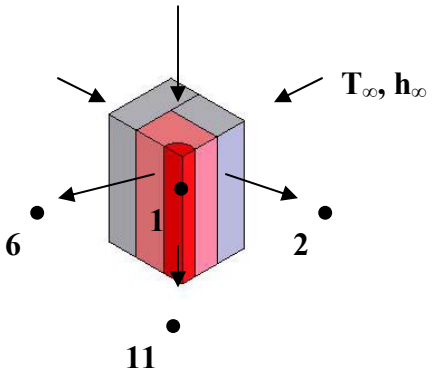

Figure 2: Nodal Analysis of Node, typical copper node

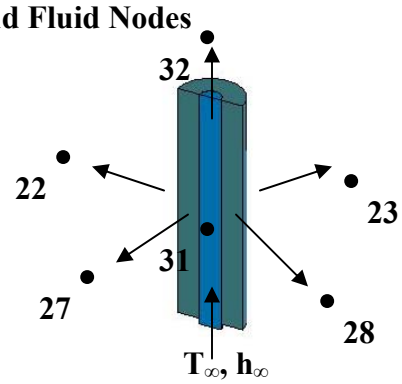

Figure 3: Nodal Analysis of Node 31 typical fluid node

Equivalent Circuit for Node 1

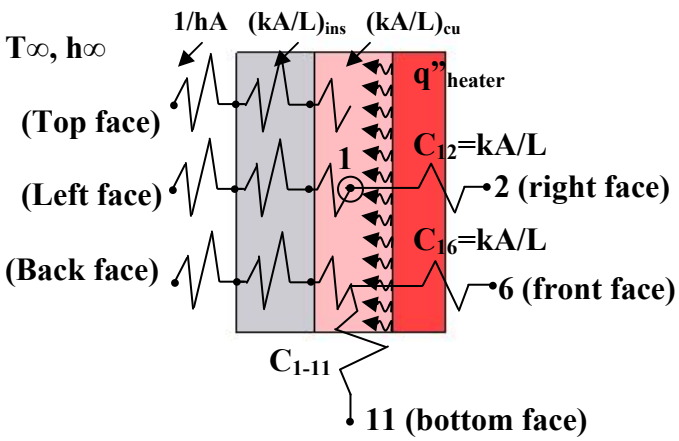

Conductance Value

$q_{12} = C_{12}\cdot(T_2-T_1) = kA/\Delta x\cdot(T_2-T_1)$

$q_{16} = C_{16}\cdot(T_6-T_1) = kA/\ \Delta y\ \cdot(T_6-T_1)$

$q_{1\text{-}11} = C_{1\text{-}11}\cdot(T_{11}-T_1) = kA/\Delta z\ \cdot(T_{11}-T_1)$

$q_{1\text{-}\infty} =(1/(hA)_{air} + (kA/\Delta x)_{ins} + (kA/\Delta x)_{cu})^{-1}(T_\infty-T_1)$

therefore: $q_{out} = q_{ij}=\Sigma C_{ij}\cdot(T_{ji})$

Energy Balance Equation

$E_{in}= E_{out} + E_{stored}$

$q_{in}= q_{out} + q_{stored}$ ← q_{out} is the sum of all the outgoing conductances

$(\rho cV)_{cu}\cdot\frac{dT}{dt} = \Sigma C_{ij}\cdot(T_{ji}) + (q''\cdot A)$ ← dT/dt simplifies to $\Delta T/\Delta t$

q_{stored}= to amount of heat loss from heater

$(\rho cV)_{cu}\cdot\frac{\Delta T}{\Delta t} = \Sigma C_{ij}\cdot(T_{ji}) + (q''\cdot A)$

$\Delta T = \frac{\Delta t}{(\rho cV)_{cu}}\cdot[\Sigma C_{ij}\cdot(T_{ji}) + (q''\cdot A)]$ ← ΔT is equivalent to change in temperature over time

$T_{final} - T_{inital} = T_f - T_i$

$T_f - T_i = \frac{\Delta t}{(\rho cV)_{cu}}\cdot[\Sigma C_{ij}\cdot(T_{ji}) + (q''\cdot A)]$

$T_f = T_i + \frac{\Delta t}{(\rho cV)_{cu}}\cdot[\ \Sigma C_{ij}\cdot(T_{ji}) + (q''\cdot A)]$ ← expand $\Sigma C_{ij}\cdot(T_{ji})$

$$T_f = T_1 + \Delta t\cdot[\ C_{12}\cdot(T_2-T_1)+ C_{16}\cdot(T_6-T_1)+ C_{1\text{-}11}\cdot(T_{11}-T_1)+ (1/(hA)_{air} + (kA/L)_{ins} + (kA/L)_{cu})^{-1}(T_\infty-T_1)]$$

$$\mathbf{T_f = T_1 + \Delta t\cdot[\ kA/\Delta x\cdot(T_2-T_1)+ kA/\ \Delta y\ \cdot(T_6-T_1)+ kA/\Delta z\ \cdot(T_{11}-T_1)+ (1/(hA)_{air} + (kA/L)_{ins} + (kA/L)_{cu})^{-1}(T_\infty-T_1)]}$$

Calculations

Time step Δt

$0 < T_1\cdot(1 - \Delta t/(\rho cV)\cdot \Sigma C_{ij})$

$0 < 1 - \Delta t/(\rho cV)\cdot\Sigma C_{ij}$

$\Delta t /(\rho cV)\cdot \Sigma C_{ij} < 1$

$\Delta t < \rho cV/ \Sigma C_{ij}$ ← see list of constants on next page

$\Delta t < 0.8942\ J\cdot K / (2.5153+4.4473+0.556+2*7.96(10)^{-6}+9.956(10)^{-6})\ W\cdot K$

$\Delta t <\ 1.7\ s$

$\Delta t = 0.005s$ <<<<< 1.7s

Calculations for Node 1:

Constants		units	Differential Areas		units
k_{cu}	401	W/m · K	Aside	0.000052	m^2
k_{ins}	0.086	W/m · K	Atop	0.00002	m^2
ρ_{cu}	8933	kg/m^3	Afront	0.000065	m^3
ρ_{ins}	480	kg/m^3	V_c	0.00000026	m^3
c_{cu}	385	J/kg · K	r_{heater}	0.0015875	m
$T_{room\ temp}$	297	K	$A_{top\text{-}heater}$	1.80217E-05	m^2
T_i	297	K	$A_{side\text{-}heater}$	3.13625E-05	m^2
Δx	0.005	m	$A_{front\text{-}heater}$	4.43625E-05	m^2
Δy	0.004	m	$A_{heatersurf}$	6.48018E-05	m^2
Δz	0.013	m			
q"	130000	K			
h_∞	1.4	$W/m^2 \cdot K$			
t_{ins}	0.125	m			

Calculations for Conductances

$(\rho cV)_{cu} = (8933\ kg/m^3 \cdot 385\ J/kg \cdot K \cdot 0.00000026\ m^3)$

$(\rho cV)_{cu} = 0.8942\ J \cdot K$

$C_{12} = k \cdot A_{side\text{-}heater} / \Delta x$

$C_{12} = (401\ W/m \cdot K \cdot 3.136 \cdot (10)^{-5}\ m^2 / 0.005\ m)$

$C_{12} = 2.5153\ W \cdot K$

$C_{16} = k \cdot A_{front\text{-}heater} / \Delta y$

$C_{16} = (401\ W/m \cdot K \cdot 4.436 \cdot (10)^{-5}\ m^2 / 0.004\ m)$

$C_{16} = 4.4473\ W \cdot K$

$C_{1\text{-}11} = k \cdot A_{top\text{-}heater} / \Delta y$

$C_{1\text{-}11} = (401\ W/m \cdot K \cdot 1.80217 \cdot (10)^{-5}\ m^2 / 0.013\ m)$

$C_{1\text{-}11} = 0.556\ W \cdot K$

$Cside_{1\text{-}\infty} = Cback_{1\text{-}\infty}$ ← The conductance exiting through insulation on side and back faces of node 1 are equal

$Cside_{1\text{-}\infty} = (\ 1/(hA)_{air} + (kAside/\Delta x)_{ins} + (kA/\Delta x)_{cu}\ )^{-1}$

$C_{1\text{-}\infty} = (\ 1/(1.4\ W/m^2 \cdot K \cdot 5.2(10)^{-4}\ m^2) + (401\ W/m \cdot K \cdot 5.2(10)^{-4}\ m^2/0.005\ m) + (401\ W/m \cdot K \cdot 5.2 \cdot (10)^{-4}\ m^2/0.005\ m))^{-1}$

$Cside_{1\text{-}\infty} = 7.96(10)^{-6}\ W \cdot K$

$Ctop_{1\text{-}\infty} = (\ 1/(hA)_{air} + (kAtop/\Delta x)_{ins} + (kA/\Delta x)_{cu}\ )^{-1}$

$C_{1\text{-}\infty} = (\ 1/(1.4\ W/m^2 \cdot K \cdot 2.0(10)^{-4}\ m^2) + (401\ W/m \cdot K \cdot 2.0(10)^{-4}\ m^2/0.005\ m) + (401\ W/m \cdot K \cdot 2.010)^{-4}\ m^2/0.005\ m))^{-1}$

$Ctop_{1\text{-}\infty} = 9.956(10)^{-6}\ W \cdot K$

$\Sigma C_{ij} \cdot (T_{ji}) = C_{12} \cdot (T_2 - T_1) + C_{16} \cdot (T_6 - T_1) + C_{1\text{-}11} \cdot (T_{11} - T_1) + \Sigma(\ 1/(hA)_{air} + (kA/L)_{ins} + (kA/L)_{cu}\ )^{-1}(T_\infty - T_1))$

$\Sigma C_{ij} \cdot (T_{ji}) = 2.5153\ W/K \cdot (T_2 - T_1) + 4.4473 \cdot (T_6 - T_1) + 0.556(T_{11} - T_1) + 2*7.96(10)^{-6}\ (T_\infty - T_1) + 9.956(10)^{-6}(T_\infty - T_1))$

Equivalent Circuit for Node 31 (Fluid Node)

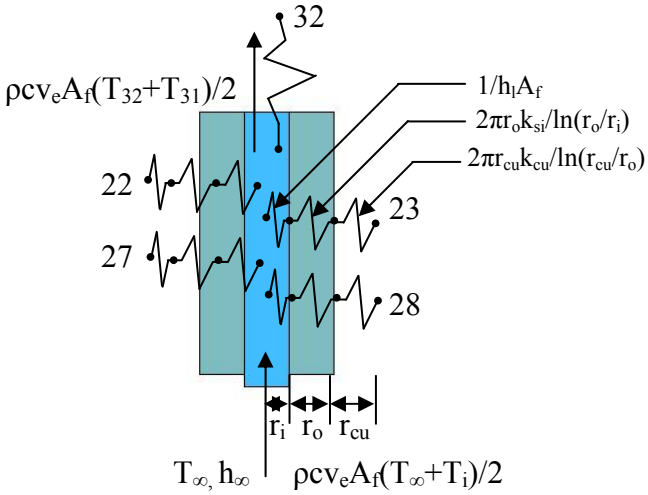

Conductance Value

$q_{31\text{-}32}=C_{31\text{-}32}\cdot (T_{32}-T_{31})$

$q_{31\text{-}32}=k\cdot A_f/\Delta z \cdot (T_{32}-T_{31}),\ \ A_f=\pi r_o^2$

$q_{31\text{-}32}=k\cdot \pi r_o^2/\Delta z \cdot (T_{32}-T_{31})$

$q_{31\text{-}22}= C_{31\text{-}22}\cdot (T_{22}-T_{31})$

$q_{31\text{-}22}=((1/(h_l\cdot A_f)+ 2\pi r_o k_{si}/\ln(r_o/r_i)$
$+2\pi r_{cu} k_{cu}/\ln(r_{cu}/r_o))^{-1}\cdot(T_{22}-T_{31})$

$C_{31\text{-}22}= C_{31\text{-}23}= C_{31\text{-}27}= C_{31\text{-}28}=$

$q_{31\text{-}cu}=C_{31\text{-}22}\cdot (T_{22}+T_{23}+T_{27}+T_{28}-4\cdot T_{31})$

$q_{31\text{-}cu}==((1/(h_l\cdot A_f)+ 2\pi r_o k_{si}/\ln(r_o/r_i)$
$+2\pi r_{cu} k_{cu}/\ln(r_{cu}/r_o))^{-1}\cdot (T_{22}+T_{23}+T_{27}+T_{28}-4\cdot T_{31})$

Enthalpy(Fluid Conductance) Values

$q_{out} = (\rho c)_l v_e A_f \cdot (T_{i+1}+T_i)/2$ ← average flow exiting

$q_{in} = (\rho c)_l v_e A_f \cdot (T_{i-1}+T_i)/2$ ← average flow entering

$q_{enthalpy} = q_{out} - q_{in}$ ← total enthalpy

$q_{enthalpy} = (\rho c)_l v_e A_f \cdot (T_{i+1}+T_i)/2 - (\rho c)_l v_e A_f \cdot (T_{i-1}+T_i)/2$

$q_{enthalpy} = (\rho c)_l v_e A_f/2 \cdot (T_{i+1}+T_i-T_{i-1}-T_i)$

$q_{enthalpy} = (\rho c)_l v_e A_f/2 \cdot (T_{i+1}-T_{i-1})$

$q_{enthalpy} = (\rho c)_l v_e A_f/2 \cdot (T_{32}-T_\infty)$ ← fluid is entering from room temperature and exiting to node 32

Energy Balance

$E_{in} = E_{out} + E_{stored}$

$q_{in} = q_{out} + q_{stored}$, $q = q_{cond} + q_{enthalpy}$

$(q_{cond} + q_{enthalpy})_{in} = (q_{cond} + q_{enthalpy})_{out} + \cancel{q_{stored}}$ ← no energy is stored, total enthalpy is in eqn. above

$(q_{cond})_{in} = (q_{cond})_{out} + q_{enthalpy}$

$(\rho c)_l v_e A_f dT/dt = q_{31\text{-}32} + q_{31\text{-}cu} + q_{enthalpy}$ ← Dt/dt is equal to $\Delta T/\Delta t$

$(\rho c)_l v_e A_f \, \Delta T/\Delta t = q_{31\text{-}32} + q_{31\text{-}cu} + q_{enthalpy}$

$\Delta T = \Delta t/(\rho c)_l v_e A_f \cdot (q_{31\text{-}32} + q_{31\text{-}cu} + q_{enthalpy})$ ← ΔT is equal to temperature at final minus temp.initial

$T_f - T_i = \Delta t/(\rho c)_l v_e A_f \cdot (q_{31\text{-}32} + q_{31\text{-}cu} + q_{enthalpy})$ ← T_i is equal to T_{31}

$T_f = T_{31} + \Delta t/(\rho c)_l v_e A_f \cdot (q_{31\text{-}32} + q_{31\text{-}cu} + q_{enthalpy})$

$T_f = T_{31} + \Delta t/(\rho c)_l v_e A_f \cdot (C_{31\text{-}32} \cdot (T_{32}-T_{31}) + q_{31\text{-}cu} + (\rho c)_l v_e A_f/2 \cdot (T_{32}-T_\infty))$

$T_f = T_{31} + \Delta t/(\rho c)_l v_e A_f \cdot (C_{31\text{-}32} \cdot (T_{32}-T_{31}) + ((1/(h_l \cdot A_f) + 2\pi r_o k_{si}/\ln(r_o/r_i) + 2\pi r_{cu} k_{cu}/\ln(r_{cu}/r_o))^{-1} \cdot (T_{22}+T_{23}+T_{27}+T_{28} - 4 \cdot T_{31}) + (\rho c)_l v_e A_f/2 \cdot (T_{32}-T_\infty))$

Calculations for Node 31 (fluid node):

k_{cu}	401	W/m · K	$d_{i\text{-}silicone}$	0.0015875
k_l	0.609	W/m · K	$d_{o\text{-}silicone}$	0.0048006
$K_{silicone}$	0.83	W/m · K	$d_{o\text{-}cu}$	0.0088006
ρ_{cu}	8933	kg/m^3	$V_{silicone}$	4.21426E-07
$\rho_{silicone}$	910	kg/m^3	V_{cu}	7.2384E-09
ρ_l	8933	kg/m^3	V_{liq}	2.57182E-08
c_{cu}	385	J/kg · K	A_f	1.97832E-06
c_l	4181	J/kg · K		
$c_{silicone}$	32.71873	J/kg · K		
$T_{room\ temp}$	24	K		
T_i	24	K		
h_l	2372	W/m2· K		
Vei	0.000007			

Calculations

Time step, Δt

$0 < T_1^{\cdot}(1 - \Delta t/(\rho cV)\cdot \Sigma C_{ij})$

$0 < 1 - \Delta t/(\rho cV)\cdot\Sigma C_{ij}$

$\Delta t /(\rho cV)\cdot \Sigma C_{ij} < 1$

$\Delta t < \rho cV/ \Sigma C_{ij}$

$\Delta t < 0.9599/(8933\cdot 4181\cdot 7.0\cdot(10^{-6}) \cdot 1.978\cdot(10^{-6}))+ [((1/(2372 \cdot 1.978\cdot(10^{-6}))+ 2\pi\cdot 7.9(10^{-4}) \cdot 0.83/\ln(0.0048/0.0015875) +2\pi\cdot 0.0088\cdot 401/\ln(0.0088/0.0048))^{-1} + 0.609\cdot \pi\cdot 0.0044^2/0.013$

$\Delta t < 0.00367/ .00736$

$\Delta t = 0.005s$ <<<<< 0.5s

$(\rho c)_l v_e A_f= (8933\ kg/m^3\cdot 4181\ J/kg\cdot K)\cdot 0.000007\cdot 1.978(10^{-6})\ m^2$

$(\rho c)_l v_e A_f=0.9599$

$C_{31\text{-}cu}=((1/(h_l\cdot A_f)+ 2\pi r_o k_{si}/\ln(r_o/r_i) +2\pi r_{cu}k_{cu}/\ln(r_{cu}/r_o))^{-1}$

$C_{31\text{-}cu}=((1/(2372 \cdot 1.978\cdot(10^{-6}))+ 2\pi\cdot 7.9(10^{-4}) \cdot 0.83/\ln(0.0048/0.0015875) +2\pi\cdot 0.0088\cdot 401/\ln(0.0088/0.0048))^{-1}$

$C_{31\text{-}cu}=(1/0.00469+0.0044+36.579)^{-1}$

$C_{31\text{-}cu}=0.004$

$C_{31\text{-}32}=.609\cdot \pi (0.00079375)^2/0.013$

$C_{31\text{-}32}=0.0000927$

$q_{out}= q_{enthalpy} + q_{cond} = (\rho c)_l v_e A_f/2\cdot(T_{32}-T_\infty) +\Sigma C_{ij}T_{ji}$

$q_{out}=0.9599/2\cdot(T_{32}-T_\infty)+ 0.004(T_{22}+T_{23}+T_{27}+T_{28}-4\cdot T_{31}) +0.0000927(T_{32}-T_{31})$